International Journal of Medical, Medicine and Health Sciences
ISSN: 2517-9969
Vol:13, No:1, 2019

The Relationship of the Dentate Nucleus with the Pyramid of Vermis: A Microneurosurgical Anatomical Study

Santhosh K. S. Annayappa, Nupur Pruthi

***Abstract*—**The region of dentate nucleus is a common site for various pathologies like hematomas, tumours, etc. We aimed to study in detail the relationship of this region with the vermis, especially the pyramid using microscopic fibre dissection technique. To achieve this aim, 20 cerebellar hemispheres were studied from the 11 cerebellums. Dissection was performed using wooden spatulas and micro dissectors under a microscope following Klingler's preservation technique. The relationship between the pyramid of vermis and the dentate nucleus was studied in detail. A similar relationship was studied on the MRI of randomly selected trigeminal neuralgia patients and correlated with anatomical findings. Results show the mean distance of the lateral margin of the dentate nucleus from the midline on anatomic specimens was 21.4 ± 1.8 mm (19-25 mm) and 23.4 ± 3.4 mm (15-29 mm) on right and left side, respectively. Similar measurements made on the MRI were 22.97 ± 2.0 mm (20.03-26.15 mm) on the right side and 23.98 ± 2.1 mm (21.47-27.67 mm) on the left side. The amount of white matter dissection required to reach the dentate nucleus at the pyramidal attachment area was 7.3 ± 1.0 mm (6-9 mm) on the right side and 6.8 ± 1.4 mm (5-10 mm) on the left side. It was concluded that the pyramid of vermis has a constant relationship with the dentate nucleus and can be used as an excellent landmark during surgery to localise the dentate nucleus on the suboccipital surface.

***Keywords*—**Fiber dissection, micro neurosurgery, dentate nucleus of cerebellum, pyramid of vermis.

I. Introduction

THE cerebellum, being the largest part of the hind brain, can get affected by various pathologies both in the paediatric age group and in adults. A significant number of these pathologies affect the region of the dentate nucleus, especially hypertensive haemorrhage [1], [2], infarct [3], metastasis etc.

Dentate nucleus phylogenetically belongs to the neocerebellum and most of the functions of cerebellar hemisphere get relayed through it. Injury to the dentate nucleus causes delay in initiation and termination of movements, terminal and intentional tremor, temporal incoordination in movements that require multiple joints, and abnormalities in spatial coordination of hand and finger movements [4]. Recent studies have also shown dentate nucleus to have non-motor functions like sensory perception, cognition and motor planning which can also get affected [5]-[9].

Santhosh Kumar Annayappa is with the NIMHANS, India (e-mail: dr.san2405@gmail.com).

During surgery on the cerebellum it is important to identify anatomical landmarks [10] and locate the dentate nucleus in relation to them, so that a safe trajectory can be developed to avoid its injury. On the inferior surface, the vermis has four parts from anterior to posterior, namely the tuber, pyramid, uvula and nodule. The pyramid and uvula are the only parts of the vermis that are exposed on the suboccipital surface [10]. The pyramid forms the largest prominence on the inferior vermis [11]. On the suboccipital surface, the dentate nucleus is closest to the surface near the region of the pyramid and the uvula, hence, the pyramid bears a significance in localisation of the dentate nucleus.

Although extensive literature is available on methods of safe resection of cerebellar lesions, very few studies [11] are available which examine safe surgical entry zones to the cerebellum by studying the anatomic relations of the dentate nucleus with important landmarks on the cerebellar surface using fibre dissection technique. The relationship of the pyramid of vermis and the dentate nucleus has briefly been mentioned in a few studies [11]. However, their relationship has not been studied in detail. Hence, the objective was to study in detail the anatomical relationship of the dentate nucleus with the pyramid of vermis.

II. Materials and Methods

Twenty cerebellar hemispheres were studied from the 11 cerebellums obtained from the human cadavers donated to the Human Brain Tissue Repository (HBTR) at the Department of Neuropathology, NIMHANS, Bangalore, with the informed consent of relatives for the use of the whole brain for biomedical research and education in a prescribed HBTR consent form.

Brain specimens of patients under-55 years of age, who succumbed to road traffic accident without any visible damage or haemorrhage to the brainstem and cerebellum were chosen for this study. Specimens belonging to patients who died due to the following factors were excluded and not chosen for dissection.

- Organophosphorus poisoning,
- Suicidal hangings,
- Cerebrovascular accidents (haemorrhages, stroke, arteriovenous malformation and aneurysms) involving brainstem & cerebellum,
- Any visible gross diffuse axonal injuries involving brainstem & cerebellum,
- Any known case of neurodegeneration,

- Any known case of infections, long standing epilepsy or psychiatric cases,
- Any known case of demyelinating or auto-immune disease
- Any neurosurgical case involving brainstem & cerebellum,
- Any known/unknown white matter involving lesions,
- Any tumour involving brainstem & cerebellum,
- Any improperly or partially fixed brains, and
- Age beyond 55 years.

A. Specimen Preparation and Preservation Technique

Specimens matching the above inclusion and exclusion criteria were selected and preserved using Klingler's preservation method [12]-[14] to facilitate white matter dissection. After carefully removing the brains from human cadavers, the dura mater was stripped, and brains were fixed in a 10% formalin solution at room temperature for two months. After the fixation period, cerebellum along with brainstem was separated at the ponto-mesenchepalic junction from the whole brain, the remaining arachnoid membrane and vasculature on the cerebellar surface was removed. The specimens were then stored in a refrigerator at -15°C to -20°C for 8–10 days. Finally, before dissection commenced, the specimens were thawed in running water for one day. Specimens were stored in fresh 10% formalin between dissection procedures. However, if the period between dissection was longer, the specimens were kept frozen for at least 12 hours and thawed again before the dissection recommenced [15].

B. Dissection Technique

Before dissection, the specimen-specific surface anatomy of the cerebellum was studied in detail. Dissection of the cerebellum was performed using wooden spatulas, fine curved metal spatulas, fine forceps, and micro dissectors with 1 mm to 3 mm tips by using a surgical dissection microscope under 0.45–40X magnification (Carl Zeiss AG, Oberkochen, Germany) and a surgical suction system.

The steps of fiber dissection included removal of biventral and gracile lobule of cerebellum followed by removal of the tonsils bilaterally to clearly expose the pyramid of vermis and to facilitate the dissection of the dentate nucleus. This was followed by dissection of the white matter fibers over the dentate nucleus to establish its relationship with the pyramid of vermis (Figs. 1-3).

The most dorsal and central part of pyramid (point A), the most lateral part of pyramid on either side (point B) and the centre of the curve of dentate nucleus (point C) were identified at this stage (Fig. 4), and the following measurements were taken:

- Length of the pyramid (Fig. 5).
- Breadth of the pyramid (Fig. 6).
- Distance between point A and point B on either side (Fig. 7).
- Distance between point B and point C on either side (Fig. 8).
- Distance between point A and point C on either side (Fig. 9).
- Depth of white matter dissected to reach the dentate nucleus at the pyramidal attachment area.

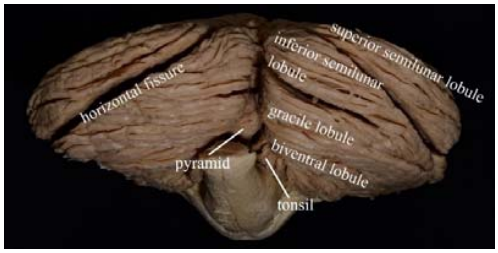

Fig. 1 Suboccipital view of the cerebellum, meninges has been stripped

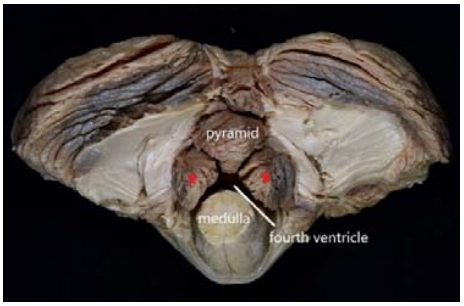

Fig. 2 Suboccipital following dissection of gracile lobule and biventral lobule, the red asterisk denotes the tonsils

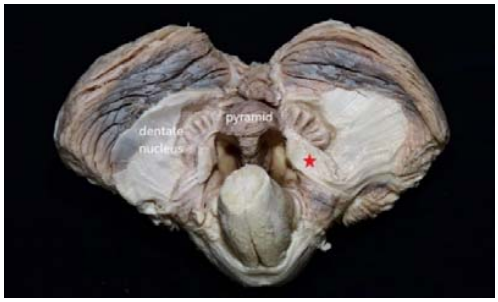

Fig. 3 Suboccipital view following dissection of gracile and biventral lobule, tonsils has been removed on both sides, the red asterisk denotes the tonsillar attachment area. The tonsillar attachment area lies on the rostral side of the basal surface of the dentate nucleus. White matter fibres have been dissected exposing the dentate nucleus and its relationship with the pyramid of vermis

Fig. 4 Point A representing the most dorsal and prominent part of the pyramid, point b representing the lateral point of the pyramid, and point c representing the lateral border of the dentate nucleus

Fig. 5 Measurement of the length of the pyramid

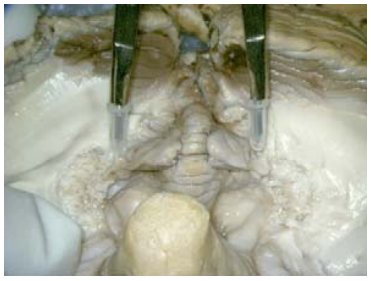

Fig. 6 Measurement of the breadth of the pyramid

Fig. 7 Measurement of the distance between point A to point B

Fig. 8 Measurement of the distance between point B to point C

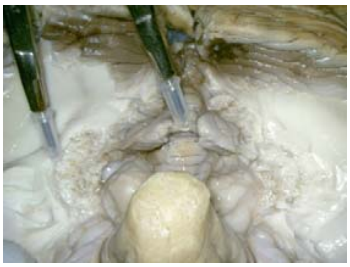

Fig. 9 Measurement of the distance between point A to point C

MRI done on 40 patients with trigeminal neuralgia were selected randomly, as in these patients, for assessment of the posterior fossa neurovascular bundle, thin slices of heavily weighted T2 image (construction interference steady state, CISS 3D) sequences were routinely performed. CISS 3D sequences were sent to OsiriX apple work station. A 3D MPR reconstruction of the axial images was done. Sagittal sequences, in which the dentate nucleus was seen most prominently was chosen, from this, the parasagittal sequence axial slices were reconstructed which went parallel to the long axis of the dentate nucleus.

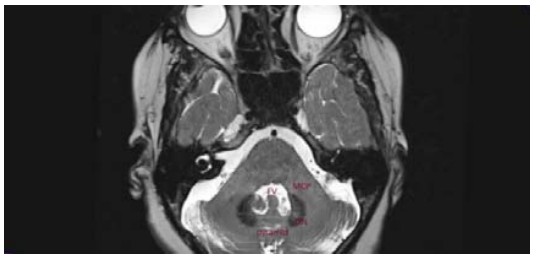

Fig. 10 Axial view on the CISS 3D MRI showing the dentate nucleus seen as a hypo intense structure. FV (fourth ventricle), DN (dentate nucleus), MCP (middle cerebellar peduncle)

From the reconstructed axial slices, the following points were selected:

A. Point corresponding to the midline of the vermis.
B. Point corresponding to the lateral extent of the pyramid, where the CSF cleft along the vermio-hemispheric fissure ends.
C. Point corresponding to the lateral most limit of the dentate nucleus along its curve.

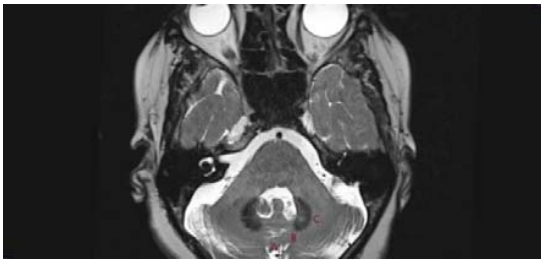

Fig. 11 Point A corresponding to the midline of vermis, point B corresponding to the lateral extent of the pyramid, where the CSF cleft along the vermio-hemispheric fissure ends, and point C corresponding to the lateral most limit of the dentate nucleus along its curve

Measurements were made to determine the following:

- Length of the pyramid.
- Breadth of the pyramid.
- Distance between point A and point B on either side.
- Distance between point B and point C on either side.
- Distance between point A and point C on either side.

III. Results

A total of 20 cerebellar hemispheres were dissected in 11 cerebellar specimens. Of the 11 specimens, in one of the specimens, the right cerebellar hemisphere was hypoplastic

and the anatomy was distorted; hence, the measurements from this hemisphere were not obtained; and of the total 20 measurements, nine were from the right side and 11 from the left side.

Of the 40 MR images that were chosen, dentate nucleus hypo intensity on CISS 3D was seen in only 15 scans. Of the 15 scans, six were female and nine were male. The mean age of the patients was 47.1 years +/- 13.41 (13-68 years).

Anatomical measurements: The suboccipital surface of the cerebellar specimens were viewed and photographed in their anatomical and surgical positions. The vermis was situated in the midline deep in the posterior incisura between the hemispheres in all the specimens, with the vermis generally getting exposed near the region of the pyramid and the uvula. The gracile lobule and biventral lobule were easily dissected along their fibres tracts and it was observed that the dissection could be done in either direction from the medial to lateral border or vice versa, and neither method had any difficulty.

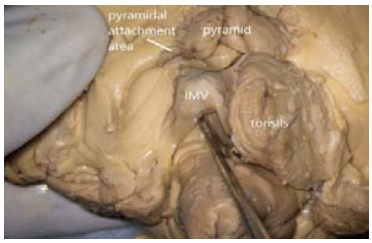

Fig. 12 Gracile lobule, biventral lobule and tonsil dissected on the left side exposing the inferior medullary velum, the pyramid of vermis seen in the midline, and the tonsils retained on the right side. The instrument points to the inferior medullary velum

In some of the early dissections, the tonsils were retained during the dissection of the dentate nucleus, but it was difficult to demonstrate the curve of the dentate nucleus reaching dentate tuberance (Figs. 2 and 3); hence, in the subsequent dissections, the tonsils were removed along its attachment. This procedure also helped to better demonstrate the relationship between the pyramid of vermis and the dentate nucleus.

Removal of the inferior medullary velum and the tela choroidae exposed the whole of the fourth ventricle along with its lateral recess (Fig. 13). The dentate tuberance which is a prominence made by the ventral part of the dentate nucleus was seen in the region of the lateral recess, on the roof of the fourth ventricle, superior and lateral to the vestibular area (Fig. 15).

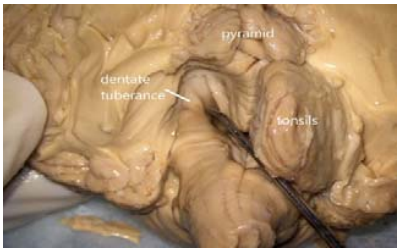

Fig. 13 Inferior medullary velum removed, exposing the lateral recess and fourth ventricle on the left side; the dentate tuberance is seen in the lateral recess of the fourth ventricle lateral to the vestibular area

It was noted that this tuberance was prominently seen on either side in seven of the 11 specimens (63.63%) and, in one specimen, it was less prominent on both sides (9.09%). In the remaining specimens, the tuberance was seen prominently only on the right side in one specimen, only on the left side in another specimen and in the one specimen only the left side was dissected, the tuberance of which was less prominent.

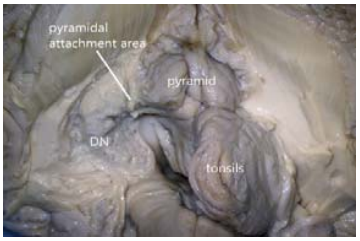

Fig. 14 Further dissection of the white matter exposing the whole of the basal surface of the dentate nucleus, relationship of the dentate nucleus with the lateral end pyramid can be appreciated. This relationship is constant in all specimens

The average breadth of the pyramid of vermis between its attachment area on either side was 21.6 +/- 2.3 mm (17-25 mm) and the length of the pyramid between the prepyramidal and secondary fissure was 19.6 +/- 1.9 mm (16-23 mm).

The mean distance measured in the anatomic specimens between the most dorsal and central part of the pyramid corresponding to the midline with the most lateral part of the pyramid corresponding to its attachment area was 13.3 +/- 1.7 mm on the right side (11-15 mm) and 13.9 +/- 1.4 mm (11-16 mm) on the left side.

TABLE I
SUMMARY OF THE COMPARISON OF MEASUREMENTS BETWEEN THE RIGHT AND LEFT SIDE ON THE ANATOMICAL SPECIMENS AND MRI IMAGES

Landmarks	Measurements	Right (mm)		Left (mm)	
		Anatomical	**MRI**	**Anatomical**	**MRI**
Distance between the midline and pyramidal attachment area	Mean	13.3	9.2	14.0	9.26
	S.D.	1.7	1.6	1.4	1.9
	Range	11-15	5.9-11.5	11-16	6.7-13.1
Distance between the pyramidal attachment area and lateral point of the dentate nucleus	Mean	9.7	13.8	10.5	14.4
	S.D.	1.7	1.9	3.0	1.9
	Range	7-12	10.4-19.2	5-15	10.7-17.6
Distance between the midline and lateral point of the dentate nucleus	Mean	21.4	22.9	23.7	23.98
	S.D.	1.8	2.0	3.4	2.1
	Range	19-25	20.0-26.1	15-29	21.5-27.7

mm = millimetre, S.D. = standard deviation

The basal surface of the dentate nucleus exposed had a constant relationship with the pyramid of vermis. Dorsally, it extended from just lateral to the pyramidal attachment area, having a gentle curve directed laterally, before reaching the roof of the lateral recess of the fourth ventricle ventrally, forming the dentate tuberance (Fig. 14).

The mean distance from the lateral most part on the dentate curve to the dorsal and most prominent part of the pyramid and the pyramidal attachment area on the right side was 21.4 +/- 1.8 mm (19-25 mm) and 9.7 +/- 1.7 mm (7-12 mm), respectively, and on the left side it was 23.4 +/- 3.4 mm (15-29 mm) and 10.5 +/- 3 mm (5-15 mm). The dentate nucleus was at a depth of 7.3 +/- 1 mm (6-9 mm) on **the** right side and 6.8 +/- 1.4 mm (5-10 mm) on **the** left side from the most lateral point of the pyramid.

MRI measurements: The CISS 3D sequence of the MRI was transferred onto the OsiriX DICOM viewer and, 3D MPR reconstruction of the images were done. The dentate nucleus was identified as a hypo intense structure in 15 of the 40 patients (37.5%); in the remaining scans, clear differentiation between the dentate nucleus and adjacent white matter could not be made out.

Following the orientation of axial slices along the long axis of the dentate nucleus on 3D MPR software, it was noted that the axial slice at which the dentate nucleus was seen most prominently, usually corresponded to the superior border of the pyramid of vermis on the sagittal images.

The mean length of the pyramid of vermis measured between the prepyramidal fissure and secondary fissure on the MRI was 13.3 +/- 2.1 mm (1.247-2.0 mm), and the breadth measured between the lateral most point on the CSF cleft corresponding to vermio-hemispheric fissure on either side was 16.1 +/- 2.0 mm (1.086-1.784 mm).

The mean distance between the most dorsal portion on the vermis corresponding to the midline to the junction of the pyramid and cerebellar hemisphere was 9.24 +/- 1.6 mm (5.8-11.48 mm) on the right side and 9.26 +/- 1.9 mm (6.71-13.05 mm) on the left side.

The mean distance between the midline and the lateral point on the curve of the dentate nucleus was 22.97 +/- 2.0 mm (20.03-26.15 mm) on the right side and 23.98 +/- 2.1 mm (21.47-27.67 mm) on the left side. The mean distance between the pyramidal attachment area to the lateral point on the curve of the dentate nucleus was 13.78 +/- 1.9 mm (10.4-19.21 mm) on the right side and 14.4 +/- 1.9 mm (10.71-17.6 mm) on the left side.

IV. Discussion

The dentate nucleus is the final common effector pathway for most of the functions of the cerebellar hemisphere. It has a ventrocaudal motor domain and a rostrodorsal non-motor domain [7], [16]. It helps in planning, initiation and coordination of motor movements, and in maintaining equilibrium and balance [17], and evidences have also shown it to have a role in cognitive function [9]. Dentate nucleus dysfunction can cause an ataxia of voluntary movements, hypotonia, dysdiadokokinesia in ipsilateral limbs and intentional tremor on voluntary movements, which can be extremely disabling to the patient.

Dentate nucleus is subjected to a range of pathological conditions like tumours, strokes, inflammatory and infective conditions, degenerative ataxias, demyelination, abnormal deposition of metabolites and toxins, drug induced toxicity and leukodystrophies [3]. Dentate nucleus is the common site for cerebellar haemorrhage secondary to hypertension, from rupture of perforating branches of the SCA and the PICA [1], [2], and it can also get affected due to ischemia in these vascular territories. It is a known entity that injury to the dentate nucleus and its efferent fibers lead to cerebellar mutism, especially in children operated for large posterior fossa tumors, particularly medulloblastoma with significant compression on the brain stem [18]. The dentate nucleus is more likely to get injured in lesions that are approached by vermian splitting and supratonsillar approaches [11], [19]–[22]. In approaches such as the telovelotonsillar and the sub tonsillar approach, the dentate nucleus remains in a safe area and is less likely to get injured [11], [22], [23]

The vermis of the suboccipital surface lies deep in the posterior cerebellar incisura, and usually gets exposed at the region of the pyramid and the uvula. The uvula is over hanged by the tonsils on either side. The pyramid forms the most prominent part of the exposed vermian surface and is so named because of its shape. Bispo et al. (2010), studied 43 cerebellums from male and female adults to determine morphological variations in the lobules of the cerebellar vermis and found the morphology of the pyramid of vermis to be constant with no variations [24]. In our study the pyramid was distinctly seen in all specimens**.** The mean length and breadth of the pyramid was noted to be 19.6 +/- 1.9 mm (16-23 mm) and 21.6 +/- 2.3 mm (17-25 mm) on the anatomical dissection and 13.3 +/- 2.1 mm (1.28-2.0 mm) and 16.1 +/- 2.0 mm (1.086-1.784 mm) on the MRI measurements, respectively. The apex of the pyramid points dorsally and slightly inferiorly with the lateral surfaces gradually tapering on either side to meet the cerebellar hemispheres deep in the vermiohemispheric fissure. The prominent apex normally corresponds to the midline [10], [11], [25]. The distance between this point to the point where the pyramid meets the hemisphere laterally was 13.3 +/- 1.7 mm (11-15 mm) on the right side and 13.9 +/- 1.4 mm (11-16 mm) on the left side in the anatomic brain dissections. Similar measurements on the MRI were 9.24 +/- 1.6 mm (5.8-11.48 mm) on right side and 9.26 +/- 1.9 mm (6.71-13.05 mm) on left side.

The transition between the vermis and hemisphere is smooth on the tentorial surface but interrupted on the suboccipital surface by vermio-hemispheric fissure. Though there appears to be a continuity between the lobules of the vermis and hemisphere at this transition, it has been noted that few layers of the cortex may be deficient and white matter fibres can get exposed in these regions [26]. In the present study, we found that following the dissection of the gracile lobule and biventral lobule from the pyramid of vermis, the attachment area of the pyramid and the underlying white matter fibres, which are usually formed by the fibres of middle

cerebellar peduncles, get exposed. The basal surface of the dentate nucleus gets exposed on further dissection of these white matter fibres. There are very few anatomical studies in the literature discussing the position of the dentate nucleus in relation to other structures in the cerebellum. Akakin et al. [11], based on the fibre dissection of 10 cerebellar hemispheres, have described in detail the anatomical relationships of the dentate nucleus using fibre dissection technique and its surgical importance, but the part of the dentate nucleus from which the measurements have been taken has not been mentioned. In their study, it is described the pyramidal attachment area to be closely related to the dentate nucleus and is about 1.8 mm away from the medial border of the dentate nucleus; however in our study, it was noted that the dorsal end of the dentate nucleus extended medial to the pyramidal attachment area and the amount of white matter that had to be dissected to reach the dentate nucleus at the attachment area was 7.3 +/- 1.0 mm (6-9 mm) on the right side and 6.8 +/- 1.4 mm (5-10 mm) on the left side.

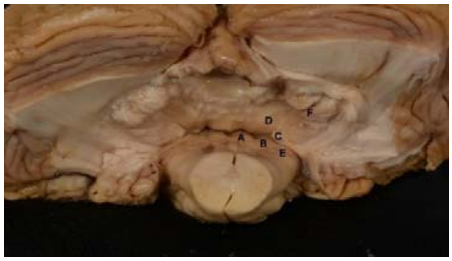

Fig. 15 The pyramid, uvula and nodule of the vermis have been removed exposing the whole of the fourth ventricle, the relationship of dentate nucleus with the cerebellar peduncles, median eminence of floor of the fourth ventricle, vestibular area can be appreciated. A (median eminence), B (vestibular area), C (dentate tuberance), D (superior cerebellar peduncle), E (inferior cerebellar peduncles), F (dentate nucleus)

Akakin et al. [11] mentioned that the lateral border of the dentate nucleus is about 17 mm from the midline; but, this measurement is made on the tentorial surface, at the plane of the tentorial fissure. Ramos et al. [10] noted that the lateral border of dentate nucleus was around 19 mm lateral to the midline, but these observations are made on cross sections of cerebellum and not on specimens dissected by fibre dissection technique. In our study, we found that the distance between the lateral border of the dentate nucleus and the prominent point on the pyramid of vermis in the midline to be about 21.4 +/- 1.8 mm (19-25 mm) on the right side and 23.7 +/- 3.4 mm (15-29 mm) on the left side, and the distance between the lateral border of the dentate nucleus with the pyramid attachment area to be 9.7 +/- 1.7 mm (7-12 mm) on the right side and 10.5 +/- 3.0 mm (5-15 mm) on the left side. Ramos et al. [10] mentions the tonsillar implantation area to correspond to the middle level of the dentate nucleus; but in our study, we found that the implantation area of the tonsils was more towards the rostral part of the basal surface of the dentate nucleus and not the middle level.

Dentate tuberance is an important landmark when approaching tumours of the fourth ventricle. It is situated superolateral to the superior vestibular area, superior to the inferior cerebellar peduncle and lateral to the median eminence at the lateral recess of the fourth ventricle. The flocculonodular lobe attachment area is closely related to the dentate tuberance and is 2.9 mm away from it [11]. In our study, dentate tuberance was seen prominently in 80% of the hemispheres dissected. The insertion of the inferior medullary velum on the hemisphere is close to the dentate tuberance. In the cerebellomedullary fissure approach to lesions in the region of the lateral recess, identification of this tuberance is important to avoid injury to the dentate nucleus [27], [28].

The dentate nucleus appears hypo intense on the T2-weighted images, due to the iron deposition that is seen in the nuclei [29], [30], [39], [40], [31]–[38]. The deposition of iron in the dentate nucleus begins by 3-7 years with peak deposition before the second decade, followed by a second peak of deposition in the fifth decade [32], [40]. MRI scans of patients with trigeminal neuralgia were selected to study the dentate nucleus in our study because, thin cut CISS 3D sequences of the posterior fossa is routinely done in these patients to view the neurovascular bundle. Also, trigeminal neuralgia generally manifests in the fourth and fifth decade, by which time the iron deposition in the dentate nucleus would be complete.

In our study, out of the 40 MRI scans of patients with trigeminal neuralgia that were chosen, dentate nucleus hypo-intensity was seen in 15 patients only. In rest of the scans, the dentate nucleus could not be appreciated as its margins could not be delineated from the surrounding white matter, which could be due to the age-related variations in iron deposition of the dentate nucleus [31], [41].

Several MRI atlases of the cerebellum are available which identify the various cerebellar nuclei, cerebellar fissures, and lobules and their 3D relations. These studies localise the dentate nucleus sterotactically for functional studies and topographic localisation [26], [31], [35], [37], [42], but very little information can be gathered from these studies regarding the relationship of the dentate nucleus with anatomical landmarks like the midline or the pyramid of vermis. Heimburger et al. in 1965, determined the dentate nucleus to start from 5 mm lateral to the mid sagittal plane and its lateral margin to be 20 mm from the midline. These measurements were obtained from the formalin fixed human cerebellum and the calculations were applied for stereotactic lesioning of the dentate nucleus on pneumoencephalography through the lumbar route in his 12 patients of cerebral palsy [43]. Gortvai et al., based on the anatomic study of nine cerebellar hemispheres in 1974, described the location and position of the dentate nucleus for stereotactic lesioning of the dentate nucleus. In this study, the position of the dentate nucleus was similar to that described by Heimburger[44]. In our study of the MRI images, we found the lateral margin of the dentate nucleus to be 22.97 +/- 2.0 mm (20.03-26.15 mm) and 23.98 +/- 2.1 mm (21.47-27.67 mm) away from midline, and 13.78 +/-1.9 mm (10.4-19.21 mm) and 14.4 +/- 1.9 mm (10.71-17.6

mm) away from the pyramidal attachment area on the right side and left side, respectively.

Most anatomical studies are usually compared with MRI studies, especially DTI, to examine the white matter fibres [11], [45], [46] or for stereotactic localisation of the dentate nucleus for PET and other functional studies [31], [35], [37], [42]. To our knowledge there is no study in the literature which compares the measurements obtained on anatomical specimens with that of MRI measurements from a fixed anatomic landmark for localisation during surgery.

The distances of the lateral margin of the dentate nucleus from the midline were similar on the anatomic specimens and MRI scans with 21.4 +/-1.8 mm (19-25 mm) and 22. 97 +/- 2.0 mm (20.0-26.1 mm) on the right side and 23.4 +/- 3.4 mm (15-29 mm) and 23.98 +/- 2.1 mm (21.5-27.7 mm) on the left side, respectively.

However, the distance between the apex of pyramid and pyramidal attachment area, 13.3 +/- 1.7 mm (11-15 mm) on the dissection and 9.24 +/-1.6 mm (5.9-11.5 mm) on the MRI on the right side and 13.9 +/-1.4 mm (11-16 mm) on the dissection and 9.26 +/-1.9 mm (6.7-13.1 mm) on the MRI on the left side, and the distance between the pyramidal attachment area and the lateral margin of the dentate nucleus 9.7 +/- 1.7 mm (7-12 mm) on the dissection and 13.78 +/-1.9 mm (10.4-19.2 mm) on the MRI on the right side and 10.5 +/- 3.0 mm (5-15 mm) on the dissection and 14.4 +/-1.9 mm (10.7-17.6 mm) on the MRI on the left side, varied. These variations appear likely because the measurements on the MRI are taken as 2D images and the points from which the measurements are made is arbitrarily chosen, whereas on the anatomical specimens, the points between the measurements are clearly defined and the measurements obtained are 3D. Diedrichsen et al. [31] in 2010, performed, 0.5 mm thick susceptibility weighted imaging using a 7T MRI scanner on 28 healthy participants, to obtain a probabilistic atlas of the deep cerebellar nuclei. The mean volume of the dentate nucleus obtained was about 155 cc, which was twice the volume of the dentate nucleus reported in several other anatomical studies. The main reason for this difference was determined to be the isometric voxel thickness of 0.5 mm used, which was inadequate to show the single cell layers which are 0.3-0.5 mm thick in the dentate nucleus. In several of the studies which used 1 mm thick slices and lower Tesla MRI scanners, the volume calculated was even higher ranging 800 – 900 cc [37], [47]. So, determination of the dentate nucleus on the MRI depends on the spatial resolution, iron content and the MRI technique. The scans used in our study were obtained from three Tesla scanners and had a slice thickness of 0.8 mm – 1 mm, hence the exact margin of the dentate nucleus would be difficult to determine on the MRI, whereas on the anatomical dissections, the margins of the dentate nucleus can be clearly defined, giving rise to variations noted in the measurements on the anatomical specimens and MRI images.

To our knowledge no study is dedicated to examination of the relationship of the pyramid of vermis with the dentate nucleus. Some studies [11] have cursorily mentioned about this relationship but not in detail. In our study, we found the pyramid of vermis to have a constant and distinct relationship with the dentate nucleus [11], [24]; hence, it can be used as an excellent landmark to access lesions occurring in the region of the dentate nucleus such as tumours, hematoma, etc. The relationship of these lesions with the dentate nucleus and the pyramid of vermis can easily be studied on preoperative MRI. This knowledge of the position of the dentate nucleus on the preoperative imaging in collaboration with the anatomic findings will help us to prevent damage to this very important structure during surgery. A few findings of surgical importance identified in our study are the distance between the lateral margin of the dentate nucleus from the midline which was 21.4 +/-1.8 mm (19-25) and 22. 97 +/- 2.0 mm (20.0-26.1 mm) on the right side and 23.7 +/- 3.4 mm (15-29 mm) and 23.98 +/- 2.1 mm (21.5-27.7 mm) on the left side on the anatomic and MRI scans, respectively. Hence, the dentate nucleus is at a high risk of injury in vermian and paravermian lesions; lesions lateral in the hemisphere are less likely to involve the dentate nucleus. The lateral point of the pyramid had a constant relationship with the dentate nucleus, and in our study, the dorsal end of the basal surface of the dentate nucleus continued medial to the pyramidal attachment area. The depth of white matter fiber dissection that was required at this point to reach the dentate nucleus was 7.3 +/- 1.0 mm (6-9 mm) on the right side and 6.8 +/- 1.4 mm (5-10 mm) on the left side.

There are several reports in which stereotactic lesioning of the dentate nucleus has been mentioned for cerebral palsy, spasticity [43], [44], [48]; however, interest in this field diminished. Currently, stereotactic localisation of the dentate nucleus is being done for functional studies like PET. There has been a renewed interest in the region of functional neurosurgery as studies have shown deep brain stimulation of the dentate nucleus to be beneficial in essential tremors, cerebellar ataxias and stroke [49]–[52]. This article will help us provide anatomic data for developing stereotactic coordinates for localisation of the dentate nucleus for DBS in the future.

To the best of our knowledge this is the first study to show the relationship of the pyramid of vermis with the dentate nucleus in detail using fibre dissection technique.

V. Conclusion

The pyramid of vermis has a constant relationship with the dentate nucleus, and the dorsal end of the basal surface of the dentate nucleus continues medially below the pyramid of vermis. The tonsillar attachment area lies on the rostral half of the basal surface of the dentate nucleus.

The amount of white matter that is required to dissect to reach the dentate nucleus at the pyramidal attachment area is 7.3 +/- 1.0 mm (6-9 mm) on the right side and 6.8 +/- 1.4 mm (5-10 mm) on the left side.

The distance between the lateral border of the dentate nucleus and the midline at the level of the most dorsal point of the pyramid is 21.4 +/-1.8 mm (19-25 mm) on the right side and 23.7 +/- 3.4 mm (15-29 mm) on the left side on the anatomical dissections and 22. 97 +/- 2.0 mm (20.0-26.1 mm)

on the right side and 23.98 +/- 2.1 mm (21.5-27.7 mm) on the left side on the MRI measurements.

The distance between the pyramidal attachment area and lateral border of the dentate nucleus is 13.3 +/- 1.7 mm (11-15 mm) on the right side and 14.0 +/- 1.9 mm (6.7-13.1 mm) on the anatomical dissections and 9.2 +/- 1.4 mm (5.9-11.5 mm) on the right side and 9.26 +/- 1.9 mm (6.7-13.1 mm) on the left side on the MRI.

The pyramid of vermis can be used as an excellent landmark during surgery to localise the dentate nucleus on the suboccipital surface to prevent injury to this very important structure.

REFERENCES

[1] Werner H. Hermann Neugebauer, Eric Juttler, Patrick Mitchell, "Decompressive craniectomy for infarction and hemorrhage," in *Stroke: E-Book: pathophysiology, Diagnosis, and Management.*, 6th ed., L. K. S. W. James C. Grotta, Gregory W. Albers, Joseph P. Broderick, Scott E. Kasner, Eng H. Lo, A. David Mendelow, Ralph L. Sacco, Ed. elsevier, 2015, pp. 1200–1217.

[2] A. L. D. Vikram V. Nayar, "Surgical Management of cerebellar Stroke-Hemorhhage and Infarction," in *Scmidek and sweet operative neurosurgical techniques. indications, methods and results.*, 6th ed., B. L. H. Christopher S. Ogilvy, Ed. Elsevier, 2012, pp. 837–844.

[3] S. Khadilkar, S. Jaggi, B. Patel, R. Yadav, P. Hanagandi, and L. L. Faria Do Amaral, "A practical approach to diseases affecting dentate nuclei," *Clin. Radiol.*, vol. 71, no. 1, pp. 107–119, 2016.

[4] J. B. Paul w. Brazis, Joseph C. Masdeu, Ed., "The cerebellum," in *localization in clinical neurology*, 6th ed., Lippioncott Williams and Wilkins, 2001, pp. 403–418.

[5] C. J. O'Halloran, G. J. Kinsella, and E. Storey, "The cerebellum and neuropsychological functioning: A critical review," *J. Clin. Exp. Neuropsychol.*, vol. 34, no. 1, pp. 35–56, Jan. 2012.

[6] J. D. Schmahmann, "Disorders of the Cerebellum: Ataxia, Dysmetria of Thought, and the Cerebellar Cognitive Affective Syndrome," *J. Neuropsychiatry Clin. Neurosci.*, vol. 16, no. 3, pp. 367–378, Aug. 2004.

[7] R. P. Dum, "An Unfolded Map of the Cerebellar Dentate Nucleus and its Projections to the Cerebral Cortex," *J. Neurophysiol.*, vol. 89, no. 1, pp. 634–639, Oct. 2002.

[8] F. A. Middleton, "Basal-ganglia 'Projections' to the Prefrontal Cortex of the Primate," *Cereb. Cortex*, vol. 12, no. 9, pp. 926–935, 2002.

[9] J. D. Schmahmann and J. C. Sherman, "The cerebellar cognitive affective syndrome," *Brain*, vol. 121, no. 4, pp. 561–579, 1998.

[10] A. Ramos, F. Chaddad-Neto, H. L. Dória-Netto, J. M. de Campos-Filho, and E. Oliveira, "Cerebellar anatomy as applied to cerebellar microsurgical resections," *Arq. Neuropsiquiatr.*, vol. 70, no. 6, pp. 441–446, Jun. 2012.

[11] A. Akakin, M. Peris-Celda, T. Kilic, A. Seker, A. Gutierrez-Martin, and A. Rhoton, "The Dentate Nucleus and Its Projection System in the Human Cerebellum," *Neurosurgery*, vol. 74, no. 4, pp. 401–425, Apr. 2014.

[12] K. J., "Erleichterung der makroskopischen praeparation des gehirnsdurch den gefrierprozess.," *schweiz Arch Neurolpsychiatr*, vol. 36, pp. 247–256, 1935.

[13] E. Ludwig and J. Klingler, "Atlas Cerebri Humani." 1956.

[14] J. Klingler and P. Gloor, "The connections of the amygdala and of the anterior temporal cortex in the human brain," *J. Comp. Neurol.*, vol. 115, no. 3, pp. 333–369, Dec. 1960.

[15] A.-M. O. Ture U, Yasargil MG, Friedman AH, "Fiber Dissection Technique : Lateral Aspect of the Brain . Fiber Dissection Technique : Lateral Aspect of the Brain Ovid : Fiber Dissection Technique : Lateral Aspect of the Brain .," *Neurosurgery*, vol. 47, no. August, pp. 417–427, 2000.

[16] J. Voogd and T. J. H. Ruigrok, "The organization of the corticonuclear and olivocerebellar climbing fiber projections to the rat cerebellar vermis: The congruence of projection zones and the zebrin pattern," *J. Neurocytol.*, vol. 33, no. 1, pp. 5–21, Jan. 2004.

[17] P. R. Brazis PW, Biller J, Fine M, Palacios E, "Cerebellar degeneration with Hodgkin's disease: computed tomographic correlation and literature review," *Arch Neurol.*, vol. 38, no. 4, pp. 253–256, 1981.

[18] M. Pitsika and V. Tsitouras, "Cerebellar mutism," *J. Neurosurg. Pediatr.*, vol. 12, no. 6, pp. 604–614, Dec. 2013.

[19] S. K. Gudrunardottir T, Sehested A, Juhler M, "Cerebellar mutism: incidence, risk factors and prognosis.," *Childs Nerv Syst*, vol. 27, pp. 513–515, 2011.

[20] H. J. Asamoto M, Ito H, Suzuki N, Oiwa Y, Saito K, "Transient mutism after posterior fossa surgery.," *Childs Nerv Syst*, vol. 10, pp. 275–278, 1994.

[21] K. Kusano Y, Tanaka Y, Takasuna H, Wada N, Tada T and Y, "Transient cerebellar mutism caused by bilateral damage to the dentate nuclei after the second posterior fossa surgery. Case report.," *J Neurosurg.*, pp. 329–331, 25512BC.

[22] A. C. M. Mussi and A. L. Rhoton, "Telovelar approach to the fourth ventricle: microsurgical anatomy," *J. Neurosurg.*, vol. 92, no. 5, pp. 812–823, May 2000.

[23] T. Matsushima, M. Fukui, T. Inoue, Y. Natori, T. Baba, and K. Fujii, "Microsurgical and Magnetic Resonance Imaging Anatomy of the Cerebellomedullary Fissure and Its Application during Fourth Ventricle Surgery," *Neurosurgery*, vol. 30, no. 3, pp. 325–330, Mar. 1992.

[24] V. Cerebelar and T. y Variaciones, "Cerebellar Vermis: Topography and Variations," *Int. J. Morphol*, vol. 28, no. 2, pp. 439–443, 2010.

[25] M. D. Albert L. Rhoton, Jr., "cerebellum and fourth ventricle," *Neurosurgery*, vol. 47, no. 3, pp. S7–S27, 2000.

[26] E. M. Jan Voogd, "gross anatomy of the cerbellum," in *Essentials of Cerebellum and Cerebellar Disorders: A Primer For Graduate*, 1st ed., Y. S. Donna L. Gruol, Noriyuki Koibuchi, Mario Manto, Marco Molinari, Jeremy D. Schmahmann, Ed. Springer, 2013, pp. 33–38.

[27] J. H. P. Jordi X. Kellogg, "resection of fourth ventricle tumours without splitting of vermis: The cerebellomedullary fissure approach," *pediatr Neurosurg*, vol. 27, pp. 28–33, 1997.

[28] W. C. Jean *et al.*, "Subtonsillar approach to the foramen of Luschka: An anatomic and clinical study," *Neurosurgery*, vol. 52, no. 4, pp. 860–866, 2003.

[29] B. Drayer, R. Darwin, S. Riederer, R. Herfkens, and G. A. Johnson, "Magnetic Resonance Imaging of Brain Iron," *AJNR*, vol. 7, no. June, pp. 373–380, 1986.

[30] C. W. Tjoa, R. H. B. Benedict, B. Weinstock-Guttman, A. J. Fabiano, and R. Bakshi, "MRI T2 hypointensity of the dentate nucleus is related to ambulatory impairment in multiple sclerosis," *J. Neurol. Sci.*, vol. 234, no. 1–2, pp. 17–24, 2005.

[31] J. Diedrichsen *et al.*, "Imaging the deep cerebellar nuclei: A probabilistic atlas and normalization procedure," *Neuroimage*, vol. 54, no. 3, pp. 1786–1794, Feb. 2011.

[32] D. N. shigeki Aoki, Yoshitaka Okada, Kazumasa Nishimura, A. James Barkovich, Bent O. Kjos, Robert C. Brasch, "normal deposition of brain iron in childhood and Adolescence: MR imaging at 1.5 T," *Radiology*, vol. 172, pp. 381–385, 1981.

[33] R. Telford and S. Vattoth, "MR Anatomy of Deep Brain Nuclei with Special Reference to Specific Diseases and Deep Brain Stimulation Localization," *Neuroradiol. J.*, vol. 27, no. 1, pp. 29–43, Feb. 2014.

[34] Burton P. Drayer, "Basal Ganglia : Significance of Signal hypointensity on T2- weighted MR images," *Radiology*, vol. 173, pp. 311–312, 1989.

[35] A. Dimitrova *et al.*, "Probabilistic 3D MRI atlas of the human cerebellar dentate/interposed nuclei," *Neuroimage*, vol. 30, no. 1, pp. 12–25, Mar. 2006.

[36] N. Gelman *et al.*, "MR Imaging of Human Brain at 3 . 0 T : Preliminary Report on Transverse Relaxation Rates and Relation to Estimated Iron Content 1," *Neuroradiology*, no. 3, pp. 759–767, 1999.

[37] A. Dimitrova *et al.*, "MRI Atlas of the Human Cerebellar Nuclei," *Neuroimage*, vol. 17, no. 1, pp. 240–255, Sep. 2002.

[38] A. McNeill *et al.*, "T2* and FSE MRI distinguishes four subtypes of neurodegeneration with brain iron accumulation," *Neurology*, vol. 70, no. 18, pp. 1614–1619, Apr. 2008.

[39] S.-Q. Yan, J. Sun, Y. Yan, H. Wang, and M. Lou, "Evaluation of Brain Iron Content Based on Magnetic Resonance Imaging (MRI): Comparison among Phase Value, R2* and Magnitude Signal Intensity," *PLoS One*, vol. 7, no. 2, p. e31748, Feb. 2012.

[40] H. J. Brittenham GM, Farrell DE, "Magnetic susceptibility measurements of human iron stores.," *N Engl J Med*, vol. 307, pp. 1671–1675, 1982.

[41] M. Maschke *et al.*, "Age-related changes of the dentate nuclei in normal adults as revealed by 3D fast low angle shot (FLASH) echo sequence magnetic resonance imaging.," *J. Neurol.*, vol. 251, no. 6, pp. 740–6, 2004.

[42] J. D. Schmahmann *et al.*, "Three-Dimensional MRI Atlas of the Human

Cerebellum in Proportional Stereotaxic Space," *Neuroimage*, vol. 10, no. 3, pp. 233–260, 1999.
[43] C. C. W. R.F. Heimburger, "stereotactic localisation of the human dentate nucleus," *Neurology*, vol. 26, pp. 346–358, 1965.
[44] P. Gortvai and S. Teruchkin, "The Position and Extent of the Human Dentate Nucleus," *Acta Neurochir. (Wien).*, vol. 121, pp. 101–110, 1974.
[45] U. T. Cristina Goga, "The anatomy of Meyer's loop revisited: changing the anatomical paradigm of the temporal loop based on evidence from fiber microdissection," *J. Neurosurg.*, vol. 122, no. June, pp. 1253–1262, 2015.
[46] N. Salamon *et al.*, "White matter fiber tractography and color mapping of the normal human cerebellum with diffusion tensor imaging," *J. Neuroradiol.*, vol. 34, no. 2, pp. 115–128, 2007.
[47] S. C. L. Deoni and M. Catani, "Visualization of the deep cerebellar nuclei using quantitative T1 and rho magnetic resonance imaging at 3 Tesla.," *Neuroimage*, vol. 37, no. 2007, pp. 1260–6, 2007.
[48] B. G. B.Fraioli, "effects of sterotactic lesions of the dentate nucleus of the cerebellum in man," *appl. neurophysiol*, vol. 38, pp. 81–90, 1975.
[49] S. Ishizaka *et al.*, "161 Optogenetic Stimulation of Cerebellar Dentate Nucleus Promotes Persistent Functional Recovery After Stroke," *Neurosurgery*, vol. 62, pp. 218–219, Aug. 2015.
[50] M. J. Teixeira *et al.*, "Deep brain stimulation of the dentate nucleus improves cerebellar ataxia after cerebellar stroke," *Neurology*, vol. 85, no. 23, pp. 2075–2076, Dec. 2015.
[51] H. Ma *et al.*, "Resting-state functional connectivity of dentate nucleus is associated with tremor in Parkinson's disease," *J. Neurol.*, vol. 262, no. 10, pp. 2247–2256, 2015.
[52] D. C. de A. Manoel J. Teixeira, Rubens Gisbert Cury, Ricardo Galhardoni, Victor Rossetto Barboza, André R. Brunoni, Eduardo Alho, Guilherme Lepski, "Deep Brain Stimulation Of The Dentate Nucleus Improves Cerebellar Ataxia After Cerebellar Stroke," *Neurology*, vol. 85, pp. 2075–2076, 2015.